Supporting Information

Stress-Alteration Enhancement of the Reactivity of Aluminum Nanoparticles in the Catalytic Decomposition of *exo*-Tetrahydrodicyclopentadiene (JP-10)

Souvick Biswas[a], Dababrata Paul[a], Nureshan Dias[b], Kallista Kunzler[c], Musahid Ahmed[b*], Michelle L. Pantoya[c*], Ralf I. Kaiser[a*]

[a] Department of Chemistry, University of Hawai'i at Manoa, Honolulu, Hawaii 96822, United States

[b] Chemical Sciences Division, Lawrence Berkeley National Laboratory, Berkeley, California 94720, United States

[c] Mechanical Engineering Department, Texas Tech University, Lubbock, Texas 79409, United States

* Corresponding author. E-mail: mahmed@lbl.gov

michelle.pantoya@ttu.edu

ralfk@hawaii.edu

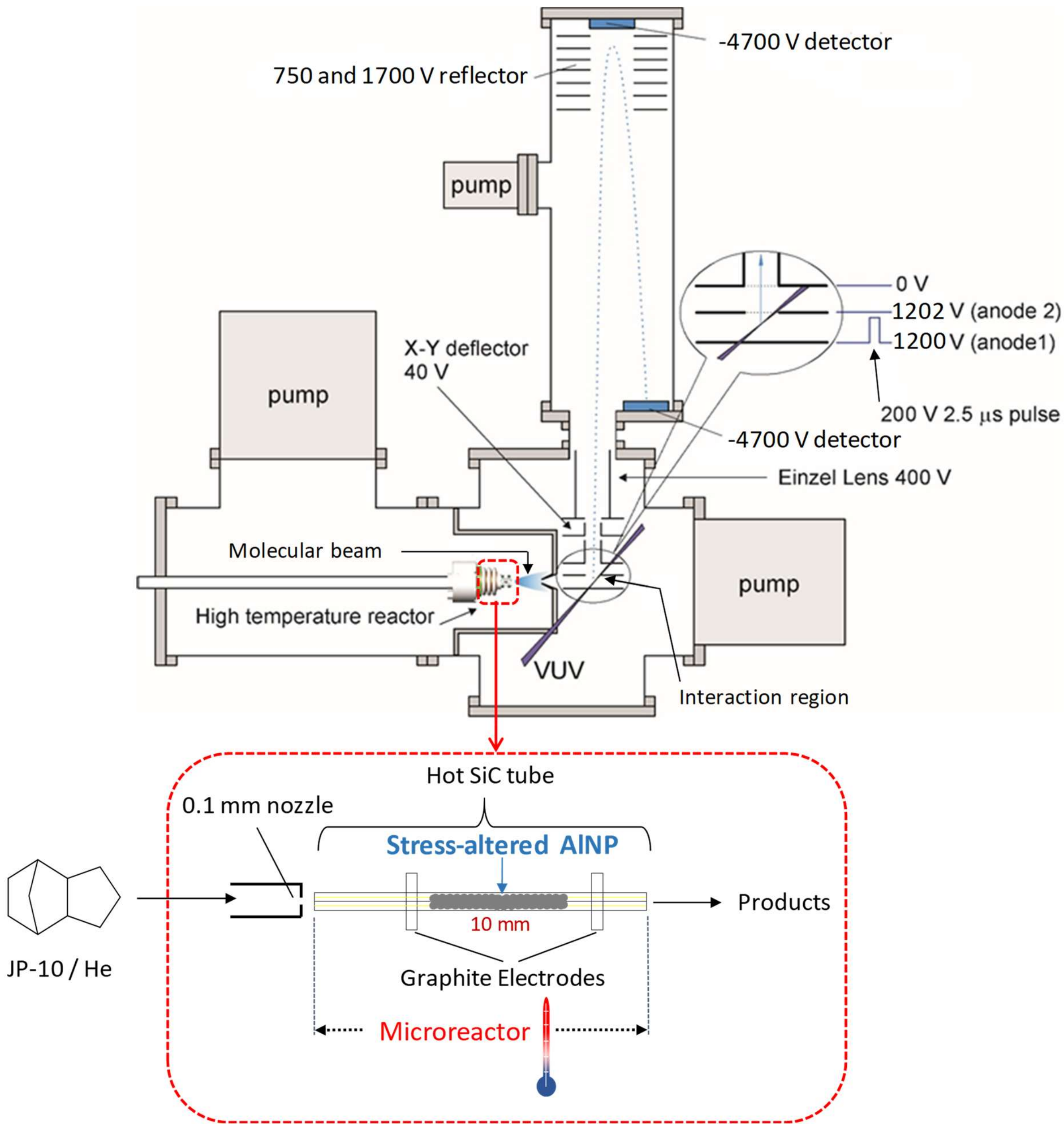

Figure S1: Schematic of the experimental setup including the catalytic microreactor and Reflectron Time-of-Flight Mass Spectrometer (Re-TOF-MS).

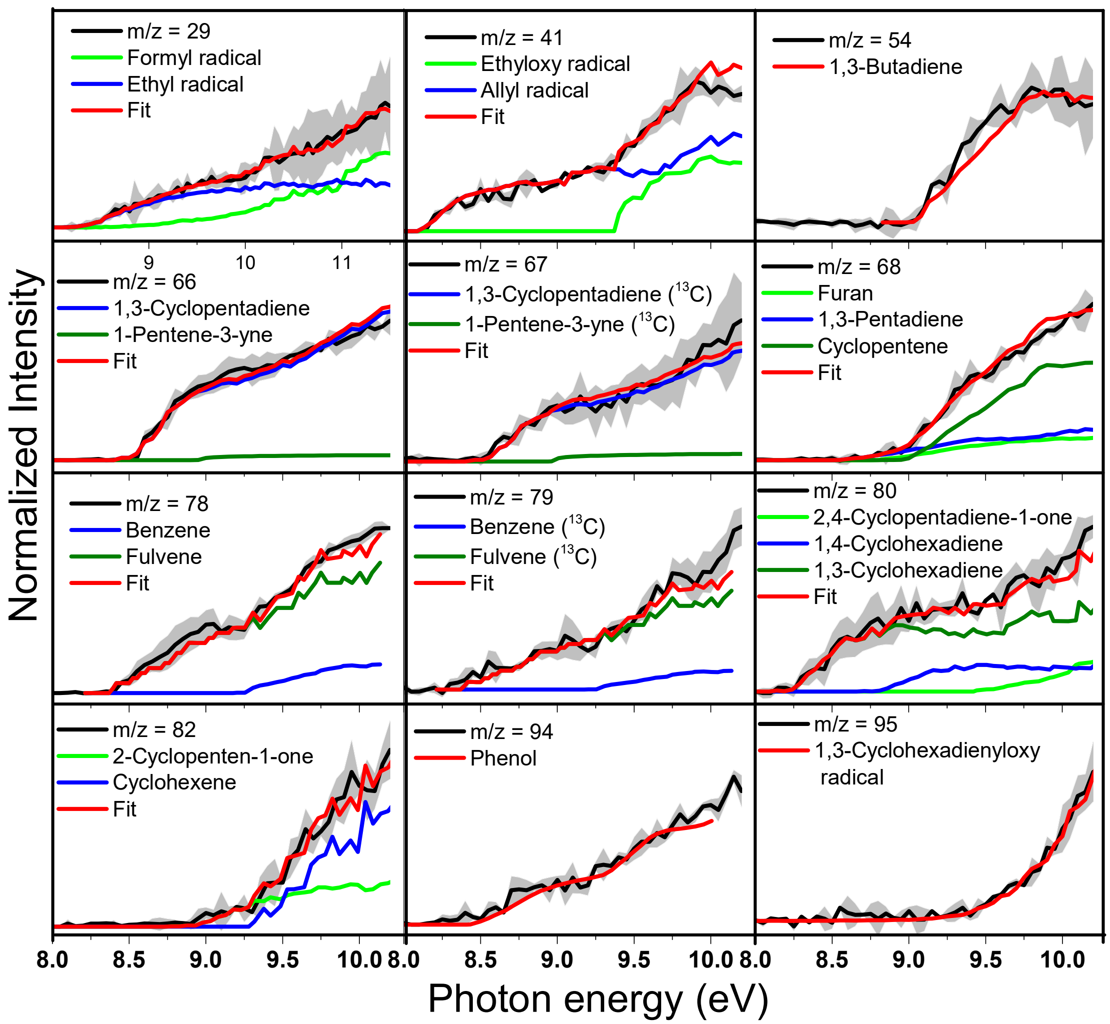

Figure S2: Experimental photoionization efficiency curves (PIE, black traces) for the products formed upon catalytic decomposition of JP-10 by stress-altered aluminum nanoparticles (SA-AlNP) at 850 K along with the experimental errors (gray shaded area) originating from the measurement errors of the photocurrent by photodiode and a 1-σ error of the PIE curves averaged over the individual scans. In case of multiple isomeric contribution, individual reference PIE curves are presented and the overall fitted curve is depicted by the red trace.

(a)

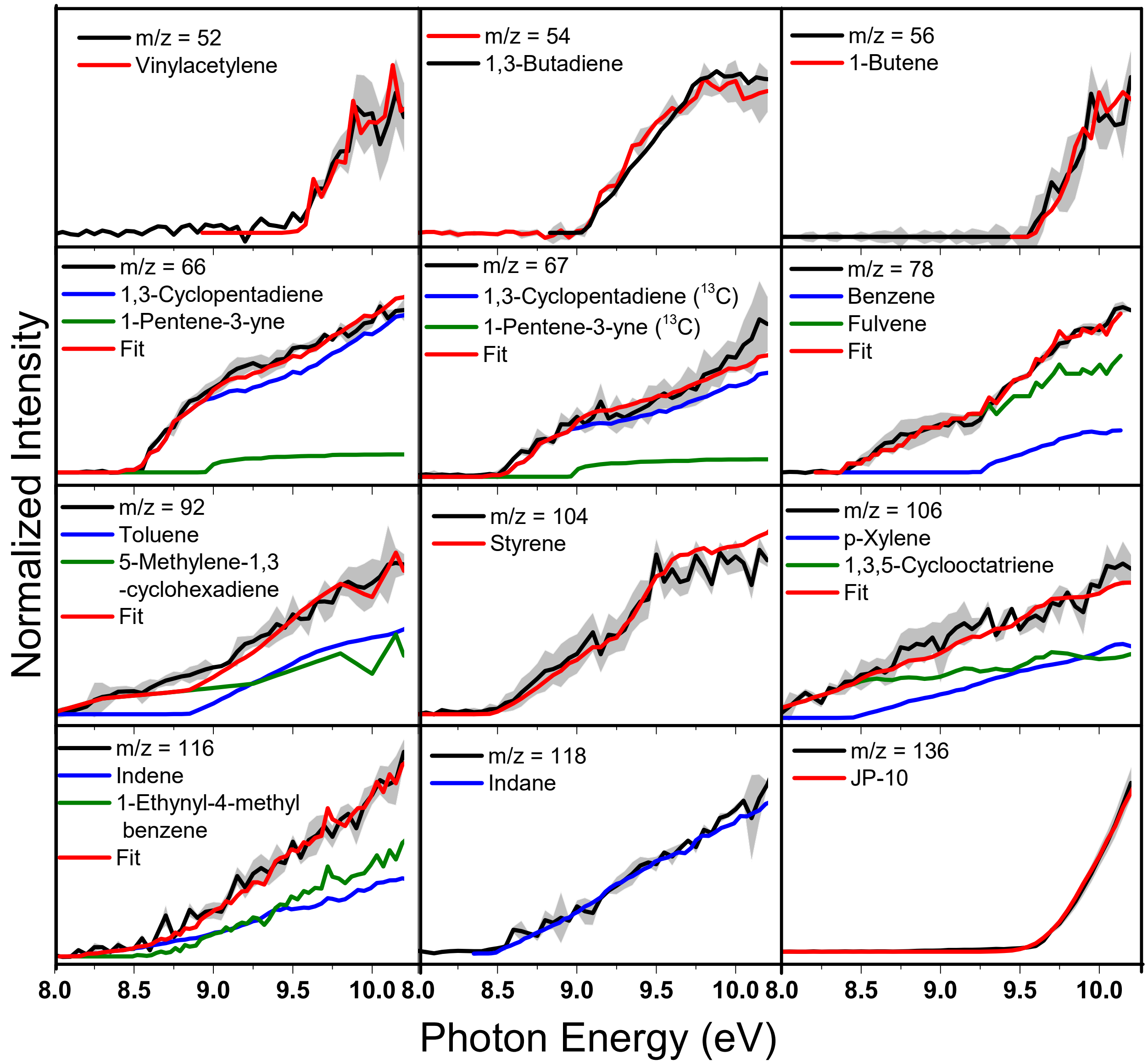

m/z = 52
Vinylacetylene
m/z = 54
1,3-Butadiene
m/z = 56
1-Butene
m/z = 66
1,3-Cyclopentadiene
1-Pentene-3-yne
Fit
m/z = 67
1,3-Cyclopentadiene (13C)
1-Pentene-3-yne (13C)
Fit
m/z = 78
Benzene
Fulvene
Fit
m/z = 92
Toluene
5-Methylene-1,3
-cyclohexadiene
Fit
m/z = 104
Styrene
m/z = 106
p-Xylene
1,3,5-Cyclooctatriene
Fit
m/z = 116
Indene
1-Ethynyl-4-methyl
benzene
Fit
m/z = 118
Indane
m/z = 136
JP-10
Normalized Intensity
8.0
8.5
9.0
9.5
10.0
Photon Energy (eV)

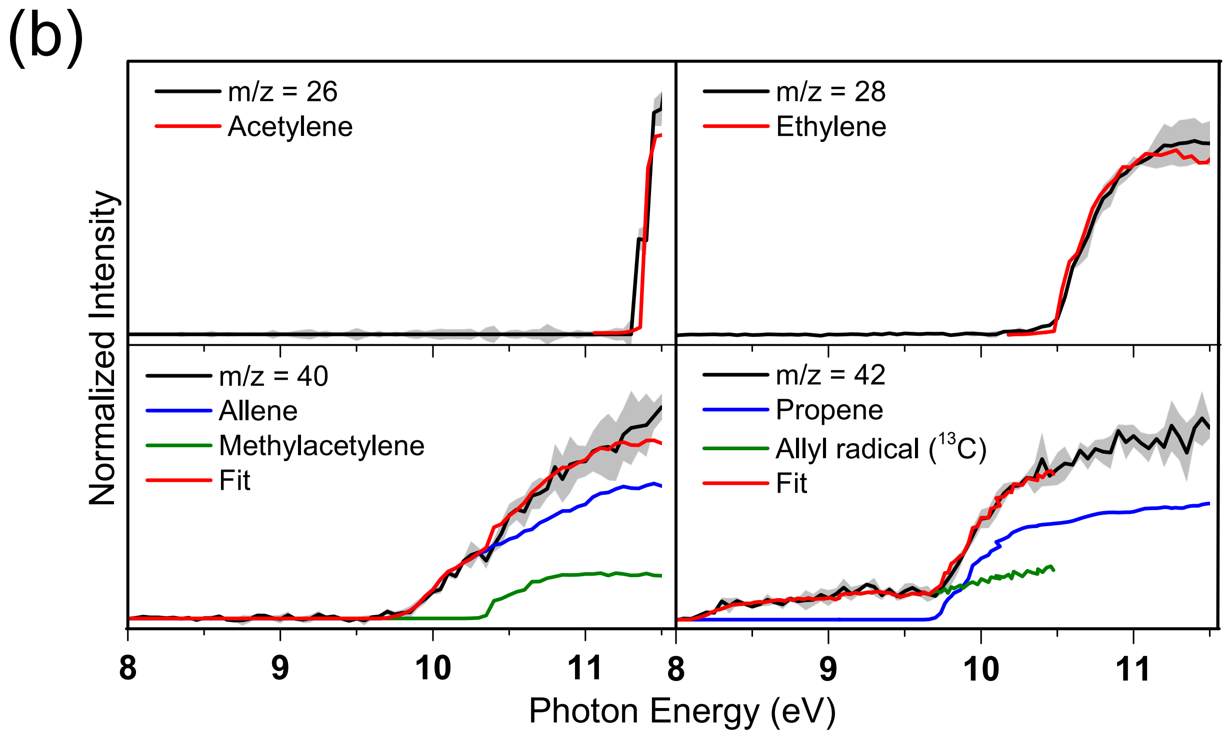

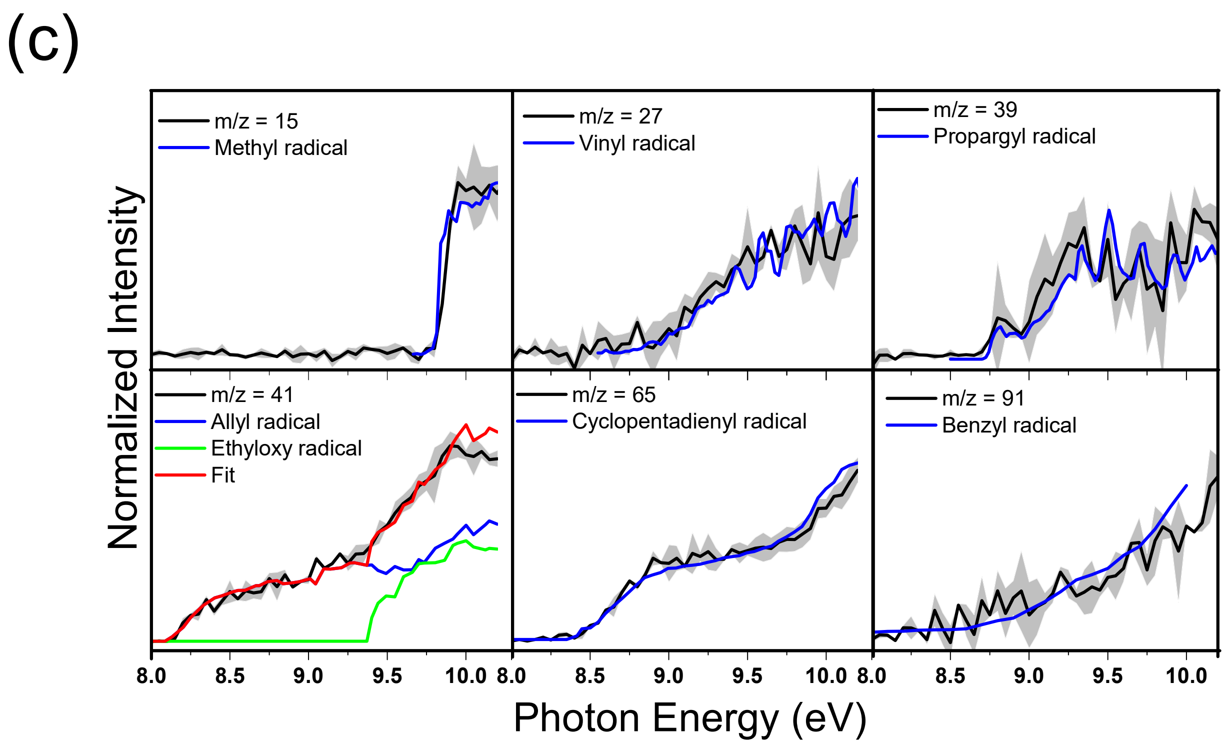

Figure S3: Experimental photoionization efficiency curves (PIE, black traces) for the (a) and (b) closed-shell hydrocarbons (olive and blue reference traces) and (c) radical products (blue reference traces) formed upon catalytic decomposition of JP-10 by the stress-altered aluminum nanoparticles (SA-AlNP) at 1,050 K along with the experimental errors (gray shaded area) originating from the measurement errors of the photocurrent by photodiode and a 1-σ error of the PIE curves averaged over the individual scans. In case of multiple isomeric contribution, individual reference PIE curves are presented and the overall fitted curve is depicted by the red trace.

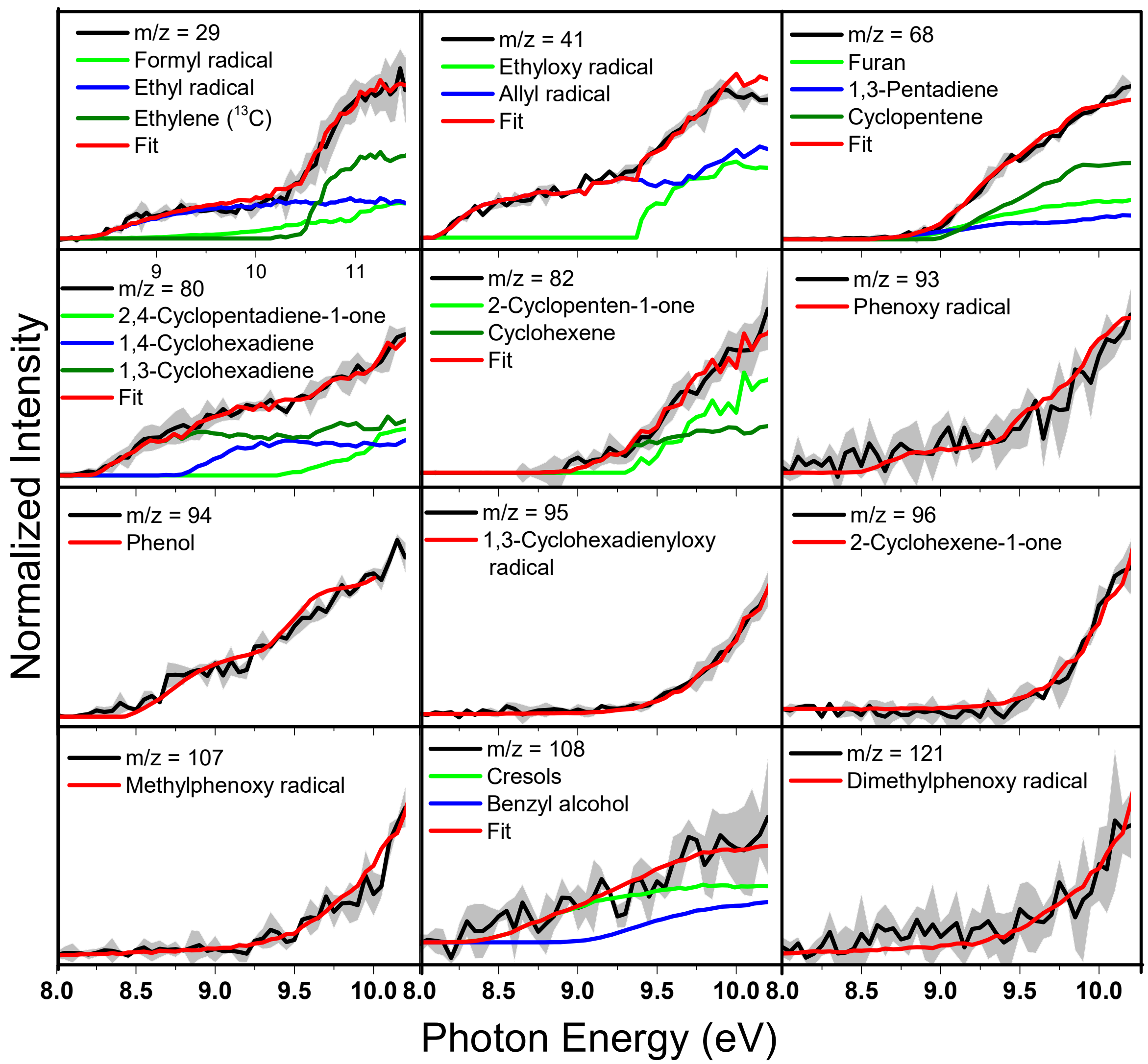

Figure S4: Experimental photoionization efficiency curves (PIE, black traces) for the oxygenated (green reference traces) formed upon thermal decomposition of JP-10 by the stress-altered aluminum nanoparticles (SA-AlNP) at 1,050 K along with the experimental errors (gray shaded area) originating from the measurement errors of the photocurrent by photodiode and a 1-σ error of the PIE curves averaged over the individual scans. In case of multiple isomeric contribution, individual reference PIE curves are presented and the overall fitted curve is depicted by the red trace.

Table S1: Compilation of the products observed in the thermal decomposition of JP-10 on untreated[1] and stress-altered AlNP, where *italicized* products are not detected in the case of the latter.

Mass	Molecular formula	Name	Structure	AlNPs	Stress-altered AlNPs
2	H_2	Hydrogen	H-H	+	+
15	CH_3	Methyl radical	$CH_3^{\cdot}$	+	+
16	CH_4	Methane	CH_4	+	+
18	H_2O	Water	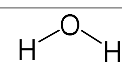	+	+
26	C_2H_2	Acetylene		+	+
27	C_2H_3	Vinyl radical	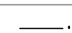	+	+
28	C_2H_4	Ethylene	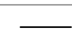	+	+
29	C_2H_5	Ethyl radical	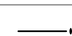	+	+
	CHO	Formyl radical	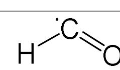	+	+
39	C_3H_3	Propargyl radical		+	+
40	C_3H_4	Allene	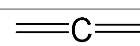	+	+
		Methylacetylene		+	+
41	C_3H_5	Allyl radical		+	+
	HC_2O	Ethyloxy radical	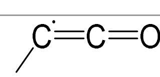	+	+
42	C_3H_6	Propene	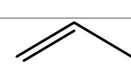	+	+

43	*AlO*	*Aluminum monoxide*	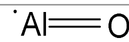	+	-
50	*C_4H_2*	*Diacetylene*	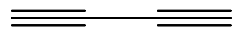	+	-
52	C_4H_4	Vinylacetylene	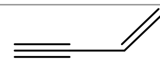	+	+
54	C_4H_6	1,3-Butadiene	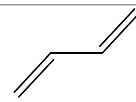	+	+
56	C_4H_8	1-Butene	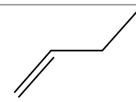	+	+
58	*C_3H_6O*	*Acetone*	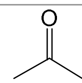	+	-
		Propanal	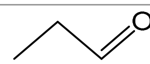	+	-
64	C_5H_4	Ethynylallene	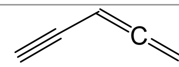	+	-
65	C_5H_5	Cyclopentadienyl radical	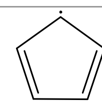	+	+
66	C_5H_6	1,3-Cyclopentadiene	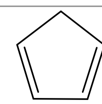	+	+
		1-Penten-3-yne	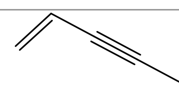	+	+
68	C_5H_8	Cyclopentene	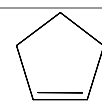	+	+
		1,3-Pentadiene	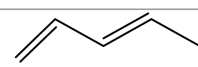	+	+
	C_4H_4O	Furan	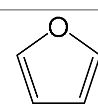	+	+
78	C_6H_6	Benzene	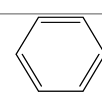	+	+
		Fulvene	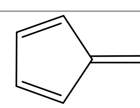	+	+
80	C_6H_8	1,3-Cyclohexadiene	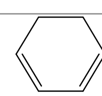	+	+
		1,4-Cyclohexadiene	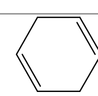	+	+

	C_5H_4O	2,4-Cyclopentadiene-1-one	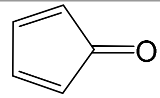	+	+
82	C_6H_{10}	Cyclohexene	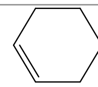	+	+
	C_5H_6O	2-Cyclopenten-1-one	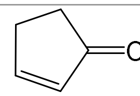	+	+
90	*C_7H_6*	*5-Ethenylidene-1,3-cyclopentadiene*	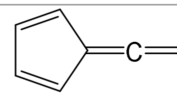	+	-
91	C_7H_7	Benzyl radical	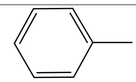	+	+
92	C_7H_8	Toluene	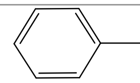	+	+
		5-Methylene-1,3-cyclohexadiene	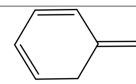	+	+
93	C_6H_5O	Phenoxy radical	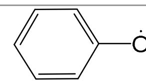	+	+
94	C_6H_6O	Phenol	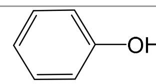	+	+
95	C_6H_7O	1,3-Cyclohexadienyloxy radical	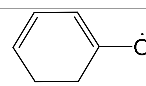	+	+
96	C_6H_8O	2-Cyclohexen-1-one	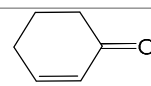	+	+
102	*C_8H_6*	*Phenylacetylene*	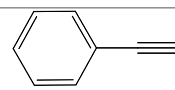	+	-
		Benzocyclobutadiene	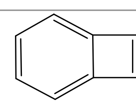	+	-
104	C_8H_8	Styrene	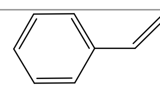	+	+
106	C_8H_{10}	p-xylene	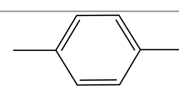	+	+
		1,3,5-Cyclooctatriene	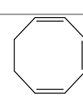	+	+

	C_7H_6O	*Benzyldehyde*	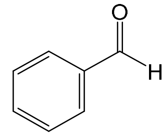	+	-
107	C_7H_7O	Methylphenoxy radical	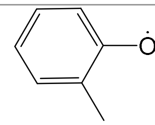	+	+
108	C_7H_8O	Cresols	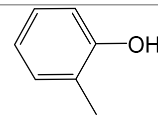	+	+
		Benzyl alcohol	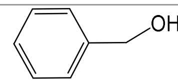	+	+
116	C_9H_8	Indene	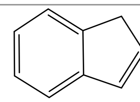	+	+
		1-Ethynyl-4-methylbenzene	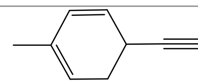	+	+
118	C_9H_{10}	Indane	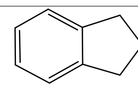	+	+
121	C_8H_9O	Dimethylphenoxy radical	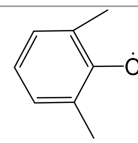	+	+
122	*$C_8H_{10}O$*	*Dimethylphenol*	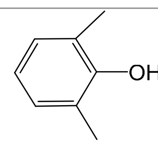	+	-
136	$C_{10}H_{16}$	JP-10	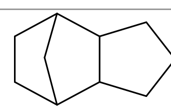	+	+

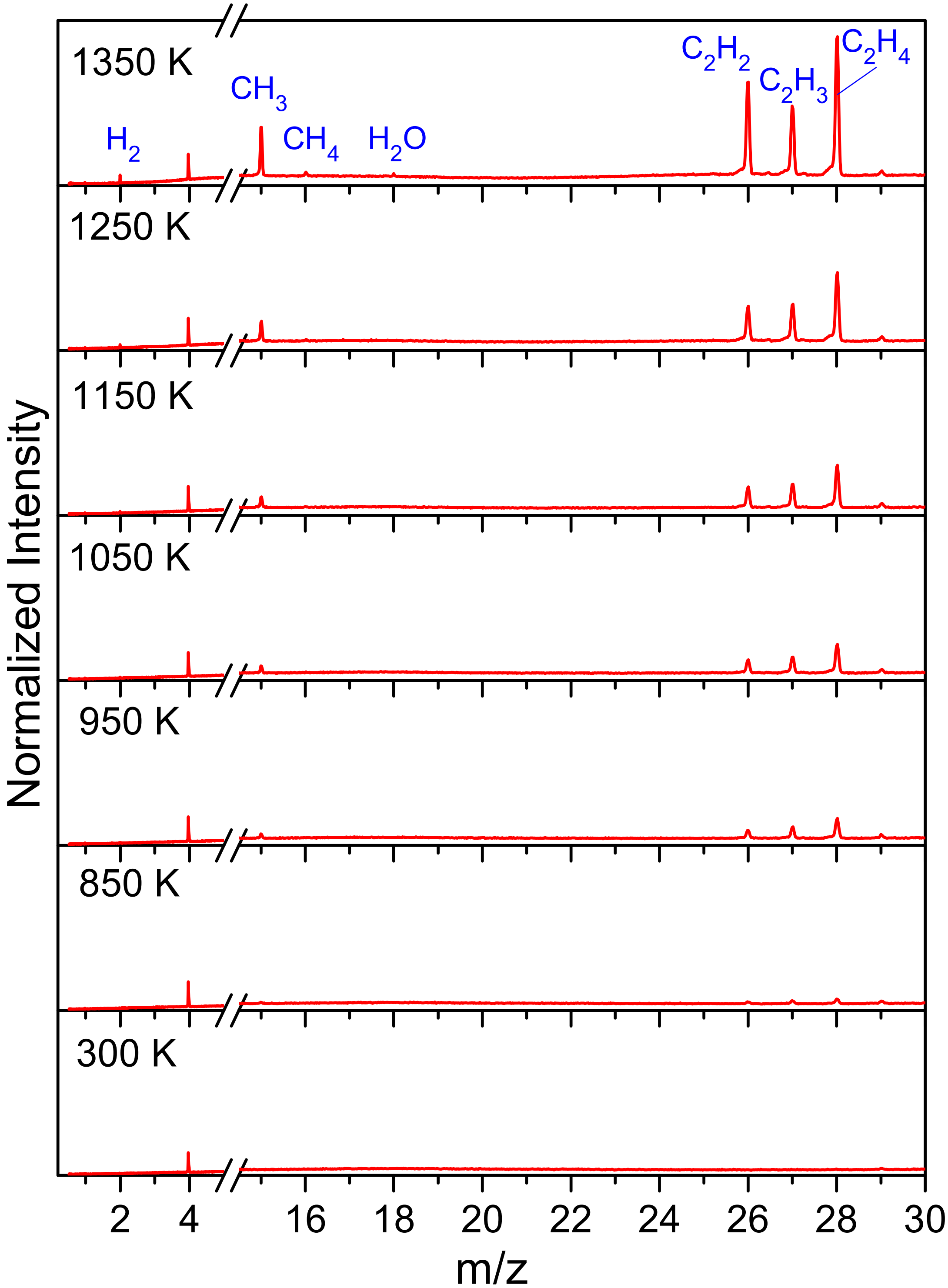

Figure S5: Mass spectra recorded at a photon energy of 15.4 eV to show a few relevant thermally decomposed products [hydrogen (H_2), methyl radical (CH_3), methane (CH_4), water (H_2O), acetylene (C_2H_2), vinyl radical (C_2H_3) and ethylene (C_2H_4)] of JP-10 vapor through stress-altered aluminum nanoparticles (SA-AlNP) in the temperature range 300 - 1,350 K.

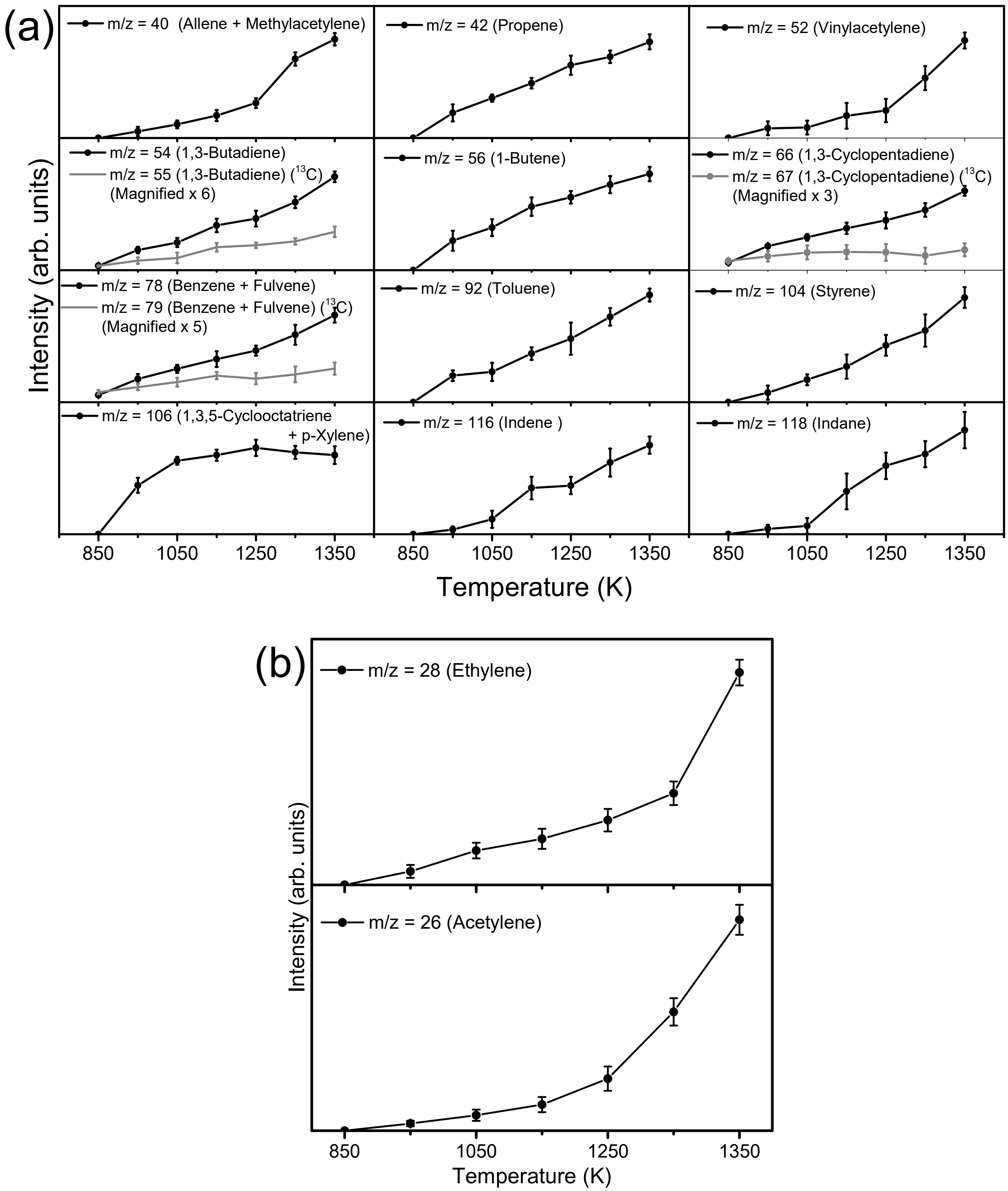

Figure S6: Temperature-dependant abundances of closed-shell hydrocarbons formed upon thermal decomposition of JP-10 on stress-altered aluminum nanoparticles (SA-AlNP) extracting the relative peak intensities from the mass spectra recorded at (a) 10 eV and (b) 15.4 eV. The error bars are due to the experimental errors of the mass peak intensities evaluated by averaging recorded mass spectra at respective photon energies (10 eV or 15.4 eV).

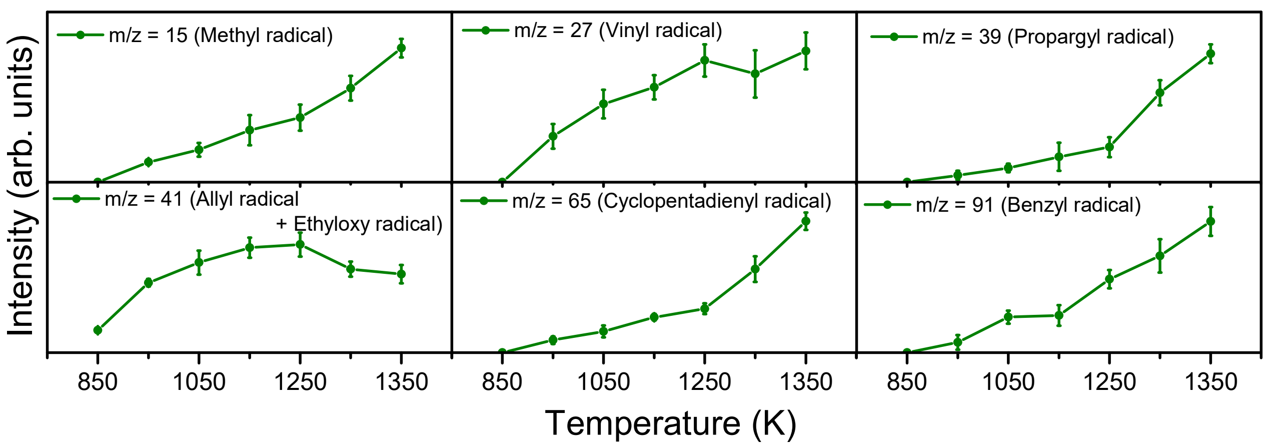

Figure S7: Temperature-dependant abundances of hydrocarbon radicals formed upon thermal decomposition of JP-10 on stress-altered aluminum nanoparticles (SA-AlNP) extracting the relative peak intensities from the mass spectra recorded at 10 eV. The error bars are due to the experimental errors of the mass peak intensities evaluated by averaging recorded mass spectra at 10 eV.

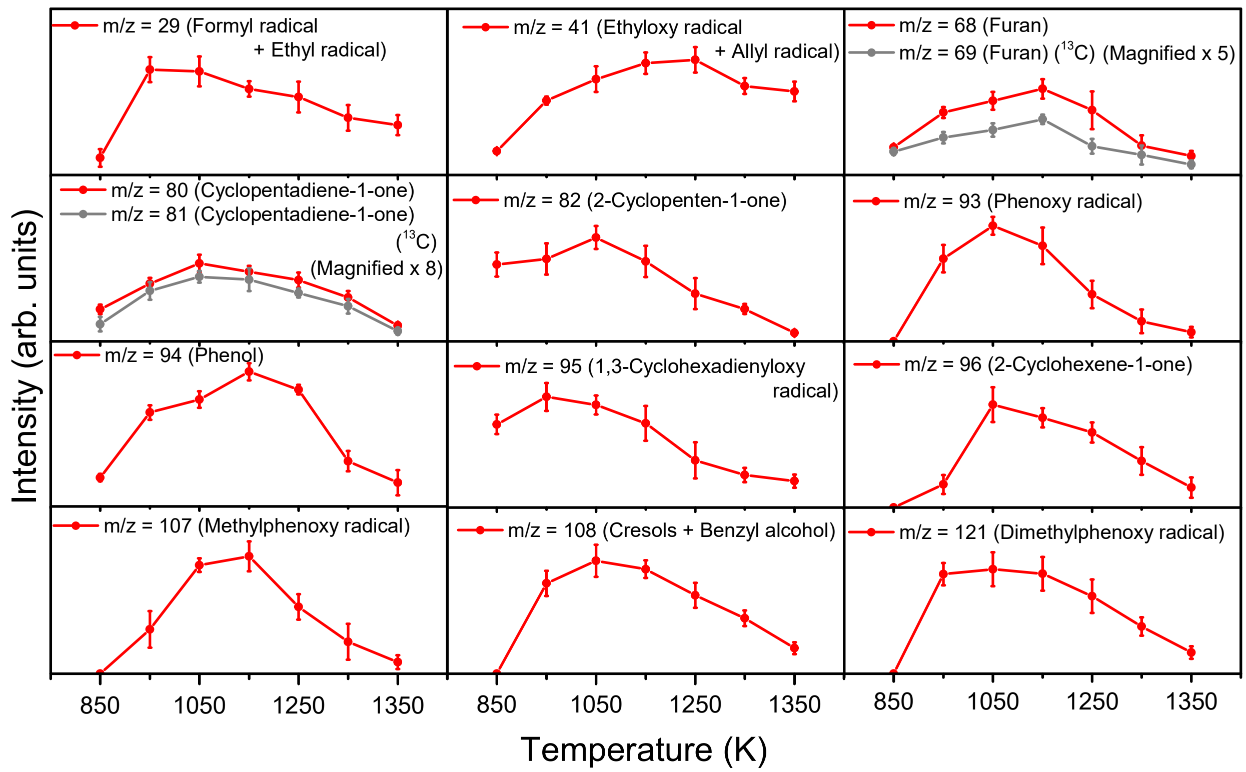

Figure S8: Temperature-dependant abundances of oxygenated products formed upon thermal decomposition of JP-10 on stress-altered aluminum nanoparticles (SA-AlNP) extracting the relative peak intensities from the mass spectra recorded at 10 eV. The error bars are due to the experimental errors of the mass peak intensities evaluated by averaging recorded mass spectra at 10 eV.

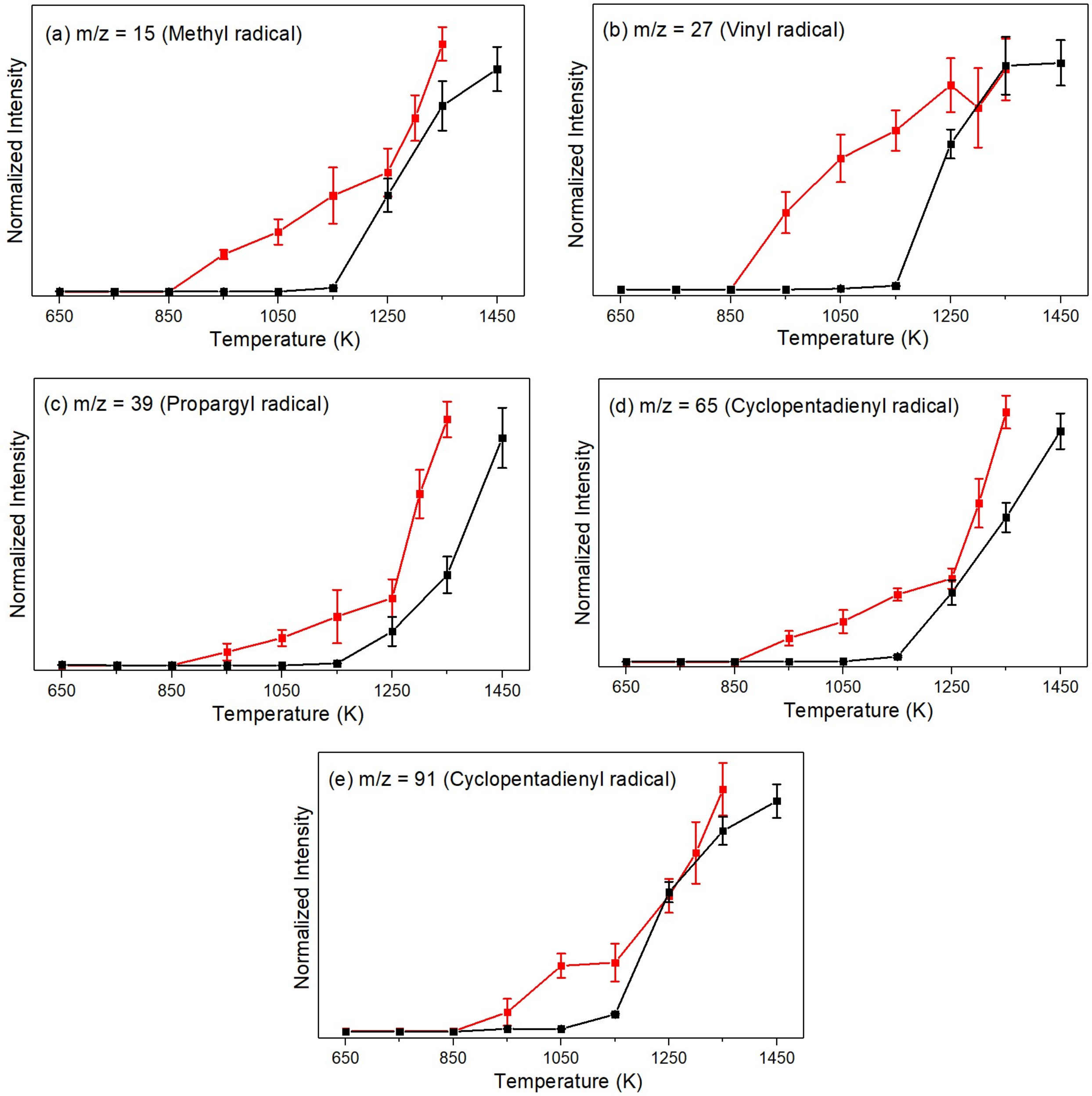

Figure S9: Comaparison of the temperature-dependant abundances of the common hydrocarbon radicals formed upon thermal decomposition of JP-10 on stress-altered aluminum nanoparticles (red traces) with those of the untreated AlNPs (black traces) extracting the relative peak intensities and transforming to a normalized scale from the mass spectra recorded at 10 eV. The error bars are due to the experimental errors of the mass peak intensities evaluated by averaging recorded mass spectra at 10 eV.